

## Chapter IV

---

### **Effect of stability on mixing in open canopies**

# **Effect of stability on mixing in open canopies**

Young-Hee Lee

Department of Astronomy and Atmospheric Sciences  
Kyungpook National University  
Daegu, 702-701, Korea

L. Mahrt\*

College of Oceanic and Atmospheric Sciences  
Oregon State University  
Corvallis, OR 97331 USA

1 June 2005

\*corresponding author: Tel: 1 541 737 5691; fax: 1 541 737 2540; email:  
mahrt@coas.oregonstate.edu

## Abstract

In open canopies, the within-canopy flux from the ground surface and understory can account for a significant fraction of the total flux above the canopy. This study incorporates the important influence of within-canopy stability on turbulent mixing and subcanopy fluxes into a first-order closure scheme. Toward this goal, we analyze within-canopy eddy-correlation data from the old aspen site in the Boreal Ecosystem - Atmosphere Study (BOREAS) and a mature ponderosa pine site in Central Oregon, USA. A formulation of within-canopy transport is framed in terms of a stability-dependent mixing length, which approaches Monin-Obukhov similarity theory above the canopy roughness sublayer.

The new simple formulation is an improvement upon the usual neglect of the influence of within-canopy stability in simple models. However, frequent well-defined cold air drainage within the pine subcanopy inversion reduces the utility of simple models for nocturnal transport. Other shortcomings of the formulation are discussed.

**Key words:** Canopy mixing, Cold air drainage, Similarity theory, Subcanopy turbulence

## 1 Introduction

The need to understand and quantify biosphere-atmosphere exchange has led to substantial interest in within-canopy turbulence. Coherent eddies encompassing the entire canopy often dominate the vertical transport and can lead to fluxes counter to the local vertical gradient within the canopy (Raupach

et al., 1996, Blanken et al., 1998, Finnigan, 2000). The primary source of canopy turbulence is often thought to be downward transport of turbulence from above the canopy.

Modelling within canopy transport normally assumes a Lagrangian or Eulerian approach. This study follows the Eulerian approach. A common modelling approach extrapolates the mixing coefficient from the surface layer above the canopy downward through the canopy using a specified functional dependence on height (e.g., Shuttleworth and Wallace, 1985; Bonan, 1996). Modelling the flux at a given level includes first-order closure (e.g., Wilson et al., 1998), K-epsilon (Katul et al., 2004), second-order closure (e.g., Poggi et al., 2004) and large-eddy models (e.g., Shaw and Shumann, 1992, Albertson et al., 2001). These models generally require a flux-gradient approximation at some level of parameterization, often expressed in terms of a mixing length (e.g., Raupach et al., 1996; Wilson et al., 1998; Katul et al., 2004; Poggi et al., 2004).

Using a mixing-layer analogy, Raupach et al. (1996) introduced the shear-length for describing turbulence above the canopy top. This length scale has been incorporated into several mixing-length formulations. For example, Wilson et al. (1998) proposed a height-dependent mixing length that approaches the shear length scale near canopy top. Poggi et al. (2004) employed a length scale related to element diameter and the distance from the ground in addition to the shear-length scale in the mixing length formulation. On the other hand, Massman and Weil (1999) focused on the influence of local leaf area index on the mixing length and related the mixing length inversely to the local drag coefficient such that the mixing length was smaller at levels with more local leaf area index.

Less attention has been given to the mixing length for momentum and

heat within open canopies and the potential role of surface heating and cooling at the ground/understory surface. Buoyancy effects in the subcanopy have been included in a few LES models (e.g. Dwyer et al., 1997; Albertson et al., 2001). Brunet and Irvine (2000) investigated the influence of stability on the shear-length scale for an open canopy and suggested that the primary effect of atmospheric stability is to modify the shear-length scale through change of wind speed and wind shear at the canopy top. However, they did not examine the influence of local stability on mixing within the canopy. Based on eddy-correlation data, Mahrt et al. (2000) found that the drag coefficient in the subcanopy at the old aspen site in BOREAS decreased with increasing subcanopy stability but did not increase from near-neutral to unstable conditions. However, they did not provide a formulation for such transport.

Much of the work above is influenced by observations of the important contribution of coherent structures to the within-canopy flux, appearing to originate above the canopy, often conceptualized in terms of within-canopy sweeps and ejection (e.g. Paw U et al. 1992). Such structures do not penetrate the strongly stratified subcanopy associated with a open overstory and clear nocturnal conditions (Mahrt, et al . 2000). In open canopies, daytime subcanopy turbulence may be generated more by local buoyancy than downward transport of turbulence from above the canopy. Resulting underestimation of subcanopy turbulence can significantly influence estimates of land-surface exchange in open canopies.

In this study, we analyze eddy-correlation data from two open canopies and construct a simple subcanopy formulation of the mixing length, which includes the influence of subcanopy stability.

## 2 Data

This study analyses eddy-correlation data collected from a mature ponderosa pine site in central Oregon, USA (Schwartz et al., 2004). Turbulent fluxes were measured above the canopy and at two levels within the canopy, one in the crown space (10 m) and one in the trunk space (3 m). The flux at 3m was measured at a subcanopy tower separated from main tower by 40 m to avoid disturbance of the flow at the tower base. Wind speed and air temperature were measured at 5 levels (3 m, 6 m, 10 m, 20 m, 30 m) on the main tower. Air temperature was also measured on the subcanopy tower at 1 m, 2 m and 3 m.

This study also analyzes tower data collected at five levels on the main tower in the old aspen site in BOREAS (Sellers et al., 1995; Blanken et al., 1997). Momentum fluxes were computed from 30-min records. The instrumentation at the old aspen site is detailed in Blanken et al. (1997). Here we include only the post leafout period when the data were the most complete.

Both canopies are characterized by a LAI of about 3 (Table 1), which we refer to as open canopies. While such values are not low compared to sparser canopies with a *LAI* of unity or less. Here, “open” refers to large diurnal variation of atmospheric stability within the canopy layer due to radiative heating and cooling of the ground/understory surface. The nocturnal temperature profiles at the old aspen site correspond to a strong surface inversion in the lowest 5 m and weaker stratification above (Mahrt et al., 2000). The stratification of the daytime aspen canopy layer is near neutral. The diurnal variation of the stratification at the pine site is much greater than that at the aspen site in spite of similar LAI values for the overstory. The strong diurnal variation of stability at the pine site is due partly to more clumping,

dryer surface conditions, less understory, higher sun angles, much less cloud cover and minimal integrable atmospheric water vapour content, all acting to increase the radiative heating and cooling of the ground surface/understory.

Fluxes are computed using deviations from 10-minute averages and then are averaged over one hour to reduce random flux errors. Fluxes in the subcanopy are subject to some uncertainty from possible flux loss due to path-length averaging and expected horizontal heterogeneity above the nonuniform understory. Based on our assessment of momentum flux loss due to path-length averaging, by comparing with three-dimensional hotfilm anemometry (unpublished), we have determined that pathlength average can lead to significant momentum flux loss in the lowest meter above short grass and that existing correction formulas are not suitable. However, we have not carried out suitable measurements in the subcanopy.

Table 1 Site description.

Sites	Average canopy height (m)	LAI	displacement height (m)	roughness length (m)
Old aspen	20.1	3.0	13.4	2.0
Pine	15.5	3.3	11	1.2

The displacement height for the aspen site (Table 1) is taken from Nakamura and Mahrt (2001) while the displacement height for the pine site was estimated by trial and error to produce the best fit to Monin-Obukhov similarity theory at the top of the tower for near-neutral conditions.

## 3 Transport in the canopy layer

### 3.1 Mixing length

We express the within-canopy flux in terms of an eddy diffusivity

$$\overline{u'w'} = -K_m \frac{\partial \bar{u}}{\partial z}, \quad (1)$$

In the data analysis below, the momentum flux will be computed as the magnitude of the vector momentum flux and the mean shear will be computed as the magnitude of the vector shear without concern for alignment of the wind and shear vectors.

The eddy diffusivity is formulated as

$$K_m = l_m u_* \quad (2)$$

where  $l_m$  is the mixing length for momentum and  $u_*$  is the height dependent friction velocity in the canopy defined as the square root of the magnitude of the momentum flux. The mixing length for momentum

$$l_m \equiv \frac{u_*}{\partial u / \partial z} \quad (3)$$

is evaluated directly from eddy-correlation and wind profile measurements at the pine and aspen sites.

The mixing length for momentum at the aspen site was computed from the observed fluxes and vertical gradients for three different stability classes, based on the stability at the top of the tower (39-m level): the unstable case ( $-1 < (z - d)/L \leq -0.1$ ), the near neutral case ( $-0.1 < (z - d)/L \leq 0.1$ ) and the stable case ( $0.1 < (z - d)/L \leq 1$ ). For this study, transition periods are eliminated and we analyze only daytime data between 1000 and 1600 local time and nocturnal data between 2100 and 0500 local time. Vertical gradients are computed from simple finite differencing.



The resulting mixing length for momentum, averaged over all of the qualifying records, increases slowly with height in the subcanopy and more rapidly with height above the canopy (Figure 1). The mixing length is much smaller in the subcanopy in stable conditions compared to neutral and unstable conditions, probably due to weaker downward transport of turbulence energy into the canopy layer. The profile of the mixing length for the pine site is based on only three levels and is not shown.

To formulate the height dependence of the mixing length, we recognize that height above the ground surface influences the within-canopy mixing while the mixing length must approach Monin-Obukhov similarity theory in the surface layer above the canopy roughness sublayer. For neutral conditions within the canopy, we propose the simple height dependence

$$l_{mn} = \beta z \quad (4)$$

where  $l_{mn}$  is the neutral value of the mixing length for momentum,  $z$  is the height above the ground surface.  $\beta$  is an empirical coefficient to-be-determined and not necessarily equal to the von Karman constant. The nondimensional coefficient  $\beta$  is estimated from the observed profiles, yielding 0.18 at the aspen site and 0.30 at the pine site. Either  $\beta$  depends on canopy architecture, or, it cannot be estimated from our observations within a factor of two.

In order that the mixing length satisfy Monin-Obukhov similarity theory in surface layer above the canopy,  $\beta$  at the top of the roughness sublayer,  $z_r$ , should approach

$$\beta = 0.4(z_r - d)/z_r \quad (5)$$

where  $d$  is the displacement height and  $z_r$  can be estimated following Raupach

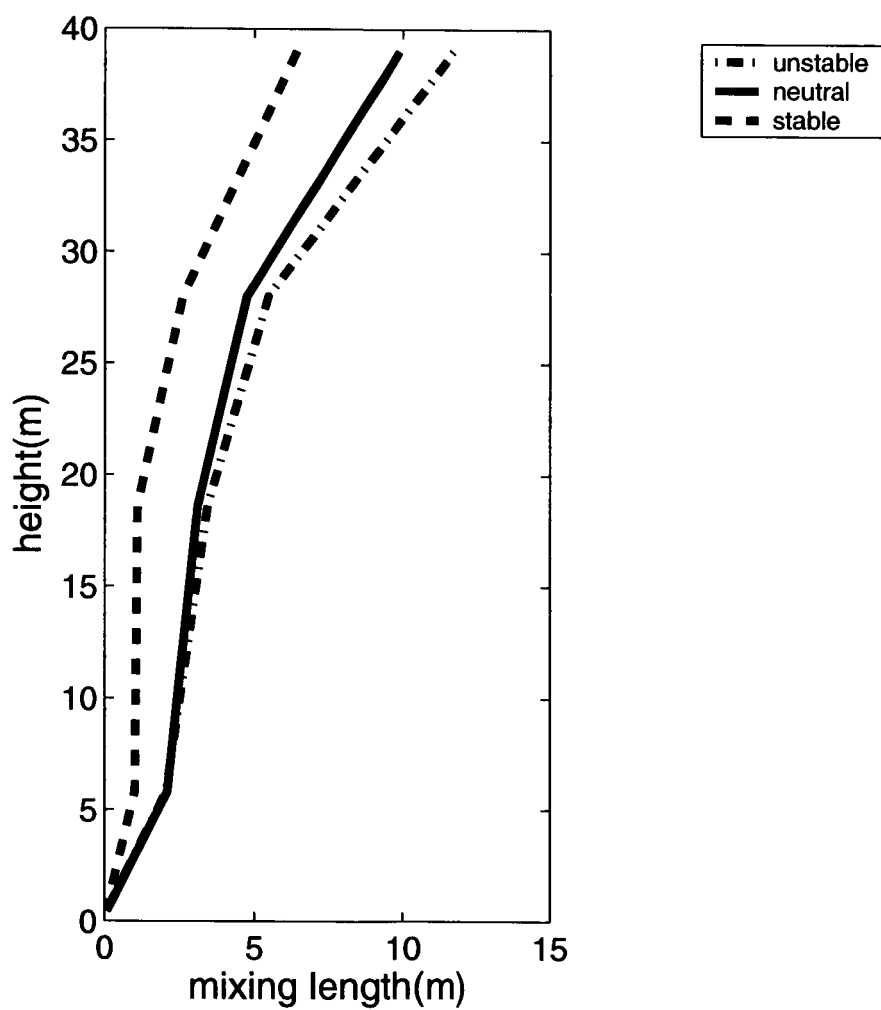


Figure 1: Height dependence of the mixing length for momentum estimated from vertical profiles at the old aspen site for the post leafout period.

(1994) as  $z_r = d + 2(h - d)$  where  $h$  is the canopy height. Assigning  $d = C h$ ,

$$\beta = 0.4[1 - \frac{C}{2 - C}] \quad (6)$$

As an exercise, we specify the displacement height to be  $2/3h$  ( $C=2/3$ ), in which case  $\beta$  becomes 0.2, which is closer to value at the aspen site. For the open canopies of this study, the value of  $C$  may be smaller leading to a somewhat larger value of  $\beta$ . Although there is no reason to expect the profile fit to Eq. 4 to agree with Eq. 6, we note that they both predict comparable magnitudes. Below, we use values of  $\beta$  from the profile fit since it avoids estimating the height of the roughness sublayer and displacement height.

### 3.2 Stability influence on momentum transfer

In analogy to Monin-Obukhov similarity theory, the stability-dependent mixing length can be expressed as

$$l_m = \frac{\beta z}{\phi_m}. \quad (7)$$

Here, the nondimensional wind shear is defined as

$$\phi_m \equiv \frac{\beta z \partial \bar{u} / \partial z}{u_*}. \quad (8)$$

We do not expect  $\phi_m$  to closely follow Monin-Obukhov similarity theory within the canopy because the stress varies rapidly with height. The flux-gradient relationship in the subcanopy will be limited in different ways by the distance from the ground surface/understory, the spacing between the trunks and the distance from the overstory. However, both the heat flux and the friction velocity are important influences so that the local Obukhov length,  $\Lambda$ , is one of the governing length scales. So that the stability approaches

Monin-Obukhov similarity theory at the top of the roughness sublayer, we formulate the subcanopy stability parameter as

$$\frac{z}{\Lambda} \left( \frac{z_r - d}{z_r} \right) \quad (9)$$

where the ratio in parentheses allows continuity of the local canopy stability functions to that above the roughness sublayer.

The nondimensional wind shear (Figures 2-3) varies more slowly with stability than predicted by the normal stability functions for Monin-Obukhov similarity theory at both the aspen and pine sites. The relationship between the nondimensional shear and stability exhibits substantial scatter, which could be due partly to the difficulty of measuring fluxes in the subcanopy (Section 2) and the omission of additional physical influences. In spite of the large scatter, inclusion of the influence of subcanopy stability is needed, although more data is required to determine the optimum stability function. The disagreement between the observations and the usual Monin-Obukhov stability functions is greatest at the lowest level of the aspen site, just above the understory, where the stability dependence is almost undetectable. Inclusion of a displacement height for the thick understory of 2-m height increases the rate at which the nondimensional shear changes with stability and thus increases the stability influence. However, this increase is not nearly large enough to allow reasonable approximation with the usual Monin-Obukhov stability functions. However, the agreement with the Monin-Obukhov stability functions improves with height (Figure 2).

The smaller observed nondimensional shear (greater mixing) for stable conditions, compared to the prediction by the usual stability functions, is presumably due to mechanical generation of mixing by the vegetation elements, not included in Monin-Obukhov similarity. However, the nondimensional shear above the canopy is also observed to be smaller than predicted

by linear dependence on stability for strong stability (e.g. Beljaars and Holt-slag, 1991; Cheng and Brutsaert, 2005). The larger nondimensional shear for unstable conditions, most evident at the pine site, could be due to the partial constraint of the convective eddies by the height of the overstory, which enters as an additional length scale not included in Monin-Obukhov similarity.

### 3.3 Stability influence on heat transfer

The pine canopy is characterized by unstable stratification (Figure 4) and significant upward heat flux in the daytime and strong stable stratification at night. The diurnal variation of the within-canopy stability is less at the aspen site as discussed in Section 2.

The heat transport is expressed in terms of the eddy diffusivity for heat

$$\overline{\theta'w'} = -K_h \frac{\partial \bar{\theta}}{\partial z} \quad (10)$$

The eddy diffusivity for heat can be related to the mixing length for heat. The mixing length for heat for near neutral conditions is difficult to estimate from data because of large scatter. We equate the neutral values of the mixing lengths for heat and momentum but allow them to have different stability functions.

The nondimensional temperature gradient is defined as

$$\phi_h \equiv \frac{\beta z \partial \bar{\theta} / \partial z}{\theta_*} \quad (11)$$

where

$$\theta_* \equiv -\frac{\overline{w'\theta'}}{u_*} \quad (12)$$

was evaluated at the two eddy-correlation levels at mature pine site, one in the crown space (10m) and the other in the trunk space (3m). This

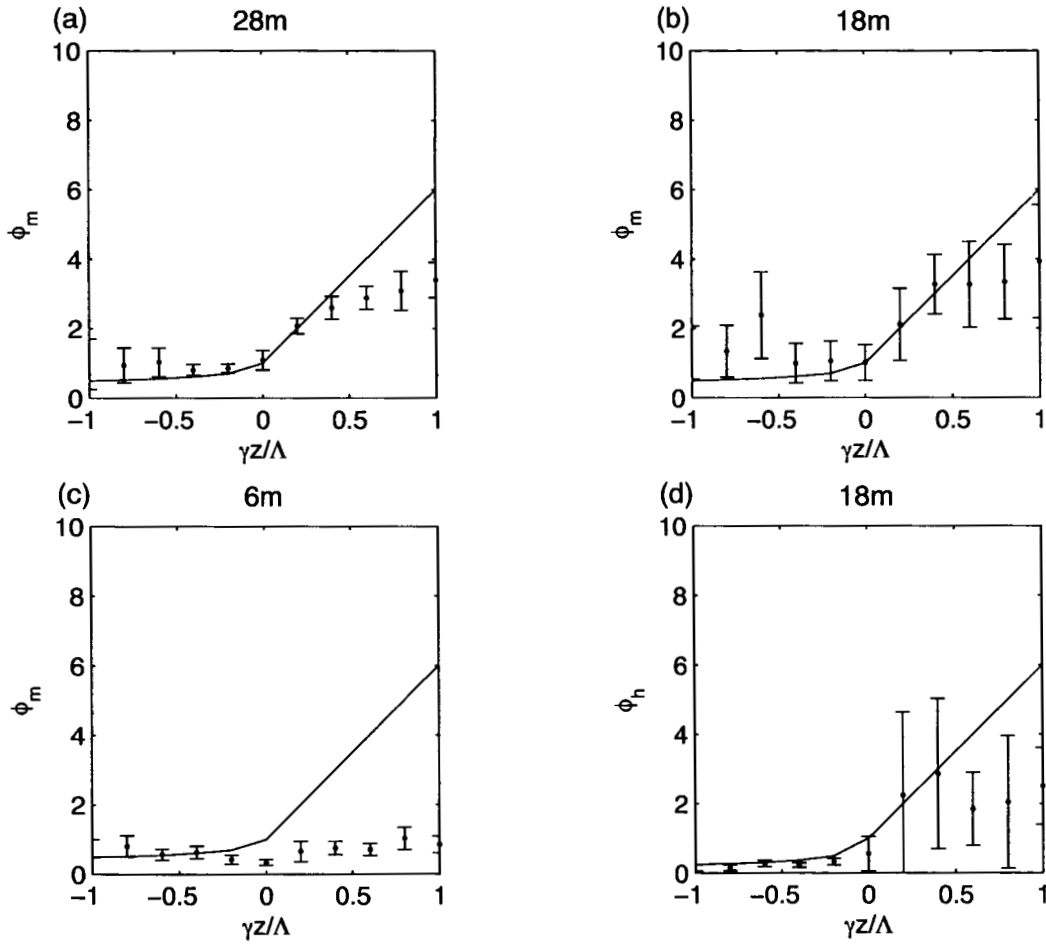


Figure 2: The nondimensional shear as a function of stability for 3 different levels at the Aspen site and the nondimensional temperature gradient at the 18-m level. The top of the canopy is approximately 20 m. The solid line corresponds to the stability function from Dyer (1974) applied to  $\gamma z/L$ , where  $z$  is the height above the ground surface.  $\gamma \equiv \frac{z_r - d}{z_r}$ .

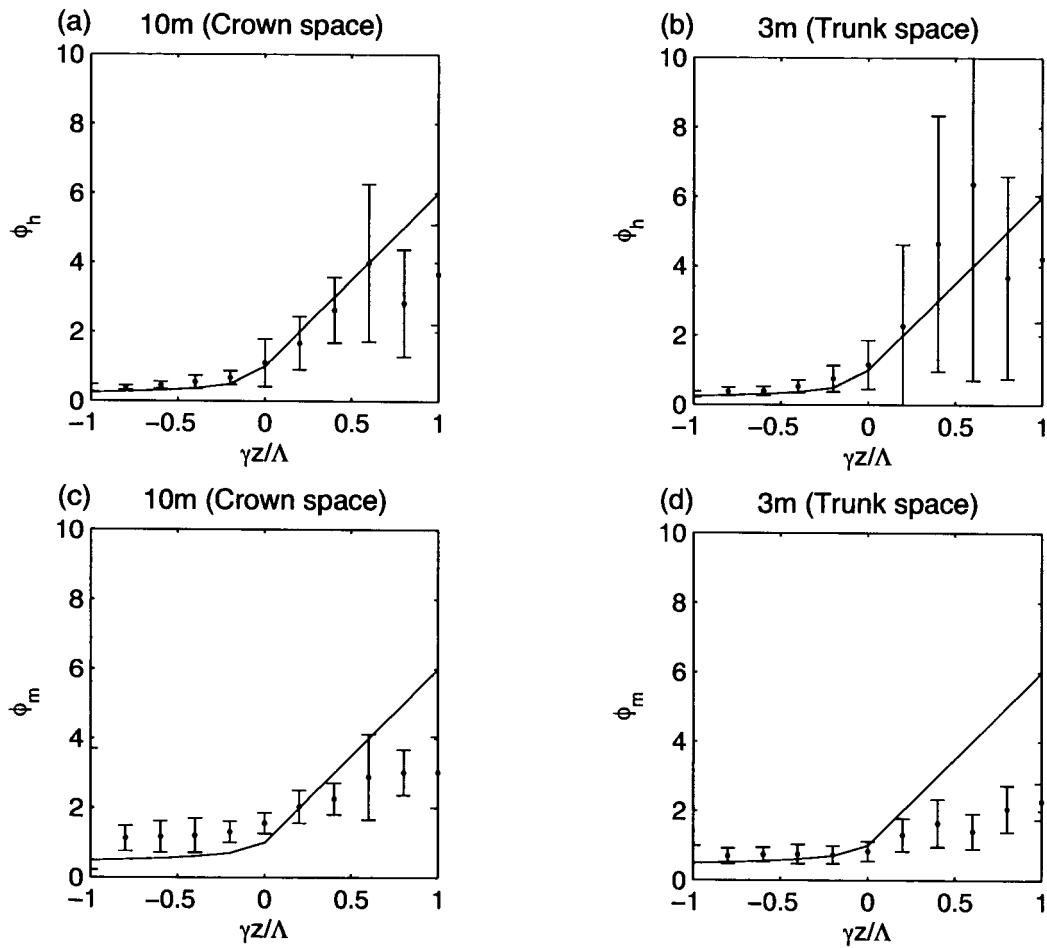


Figure 3: The nondimensional shear and nondimensional temperature gradient for two levels at the pine site. The top of the canopy is approximately 15 m. The solid line corresponds to the stability function from Dyer (1974) applied to  $\gamma z/L$ .  $\gamma \equiv \frac{z_r - d}{z_r}$ .

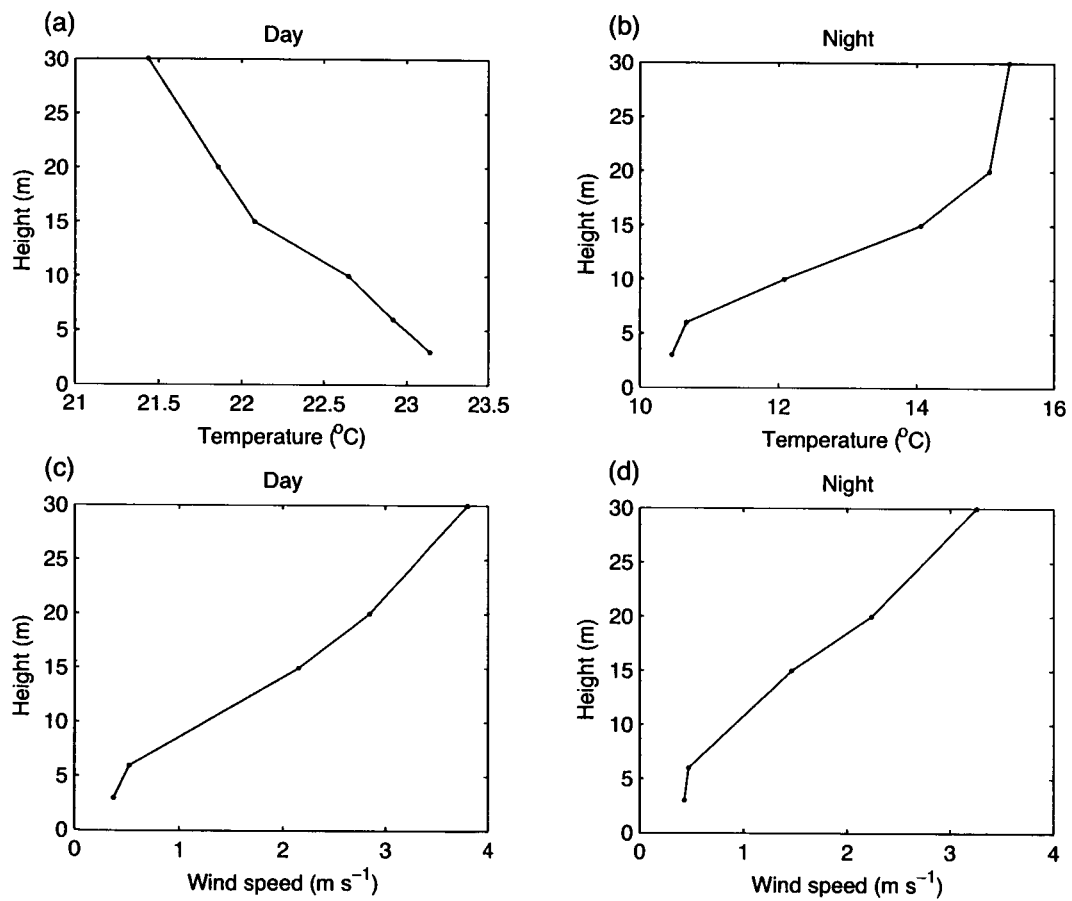


Figure 4: Averaged profiles of wind speed and temperature at the Pine site.



relationship was also evaluated at the 18-m level at the aspen site where the heat flux and vertical temperature gradients are best defined for evaluation of the relationship. Evaluation of vertical gradients must recognize that the time-averaged temperature can vary horizontally in the subcanopy on the microscale, especially close to the ground surface at the pine site. We use only data where the horizontal temperature difference at 3m between two subcanopy towers and the main tower is less than 0.5 K, which eliminates some of the most stable cases.

At the pine site, the nondimensional temperature gradient more closely follows the Monin-Obukhov stability function compared to that for momentum (Figure 3). Apparently, the influence of diabatic heating in the canopy layer and associated height-dependence of the heat flux does not strongly modify the dependence of the flux-gradient relationship on stability. However, the influence of stability on the nondimensional temperature gradient is not as well defined for the aspen site (Figure 2). At both sites, the scatter is large for stable conditions, indicating large errors in the flux calculations and/or additional influences on the nondimensional temperature gradient, not included in  $z/\Lambda$ .

Although the nondimensional temperature gradient for heat exhibits a stronger dependence on within-canopy stability compared to the nondimensional shear, the present data do not allow confident assessment of the vertical structure of the differences between the mixing lengths for heat and momentum.

With the above findings and uncertainties, we formulate the eddy diffusivity for heat as

$$K_h = \frac{l_{mn} u_*}{\phi_h} \quad (13)$$

where  $l_{mn}$  is the mixing length for momentum for neutral conditions (Eq. ??),

$u_*$  is the height-dependent friction velocity and  $\phi_h$  is the nondimensional temperature gradient with the usual Monin-Obuhkov stability functions, which formally enter here as the stability dependence of the mixing length. Since the dependence of the nondimensional shear on stability is less certain than that for temperature, we choose to follow the traditional top down approach of extrapolating the stress downward from the surface layer using a profile model. Ultimately, a separate equation for the momentum budget is needed for the canopy layer.

## 4 Influence of LAI on canopy momentum flux

Estimation of the diffusivity for heat from the stability-dependent mixing length in the previous section requires information on the mean profile of the local friction velocity in the canopy, which we now parameterize based on the observed behavior. The ratio of the subcanopy friction velocity to that above the canopy increases with increasing instability (Figure 5), presumably due to greater mixing in the daytime as suggested by larger within-canopy mixing lengths in the daytime (Figure 1). We will include the influence of the vertical structure of the  $LAI$  on the height dependence of the friction velocity. For the aspen site, the downward accumulated Leaf Area Index ( $LAI_{acc}$ ) is estimated based on the canopy structure of the aspen (Blanken et al. 1997). We then relate the momentum flux in the mean wind direction to stability and canopy architecture as

$$u_*^2 = u_{*o}^2 \exp[-2\alpha(LAI_{acc})^{0.5}] \quad (14)$$

where  $\alpha$  is a stability-dependent coefficient evaluated below and  $u_{*o}$  is the friction velocity in the surface layer above the canopy. The exponential form allows the momentum flux to approach the surface layer value above the

canopy. The square root dependence on the accumulated LAI was determined as a reasonable fit to near-neutral conditions. Although Eq. 14 adequately simulates the vertical profile of local friction velocity at the aspen site, the significant deviations of the observed from the predicted values at the pine site (Table 2) either indicate inadequate vertical resolution of the flux profiles at the pine site or imply that the local friction velocity for near-neutral conditions are affected by factors other than accumulated LAI. The pine site is characterized by greater foliar clumping and clumping of trees, allowing easier vertical exchange and greater within-canopy momentum flux compared to Eq. 14.

Table 2. Vertical profile of the height-dependent friction velocity normalized to the value above the canopy for neutral conditions. The ratio is defined as the local  $u_*$  divided by friction velocity above the canopy,  $u_{*0}$ .

Aspen site				Pine site			
z(m)	$LAI_{acc}$	Ratio		z(m)	$LAI_{acc}$	Ratio	
		observed	estimated			observed	estimated
28	0	1	1	30	0	1	1
18.6	1.	0.49	0.37	10	1.5	0.62	0.29
5.8	3.	0.19	0.18	3	3	0.13	0.18
0.45	6.5	0.05	0.08				

Using the observed fluxes, we have computed  $\alpha$  from Eq. 14. We have visually fit the stability dependence of  $\alpha$  for unstable conditions as (Figure 5)

$$\alpha = \frac{1.0}{(1 - 4z/L)^{0.25}}. \quad (15)$$

Application of this stability dependence in Eq. 14 leads to reasonable prediction of the ratio of the subcanopy stress to the stress above the canopy for

unstable conditions at both the aspen and pine sites. For stable conditions,  $\alpha$  appears to be independent of stability (Figure 5). While the above inclusion of differences between stable and unstable conditions is rather crude, it is expected to be an improvement upon the usual practice of neglecting the influence of stability on the subcanopy transport. However, with the frequent occurrence of drainage flow and capping inversion at the pine site (Section 5), the vertical communication is too weak to apply Eq. 14 and a separate time-dependent momentum equation is needed near the surface.

## 5 Nocturnal structure of the pine subcanopy

Part of the large scatter for the nocturnal flux-gradient relationship at the pine site is due to cold air drainage and wind directional shear. While some cold air drainage also occurred at the aspen site (Lee, 1998), it seemed to be less common and have less impact on the vertical structure of the flow within the canopy compared to the pine site. With cold air drainage at the pine site (westerly flow near the surface), the nocturnal stratification is much stronger and concentrated at the top of the cold air drainage, between 10 and 20 m (Figure 4). For individual hours, the stratification is often confined to a single 5-m observational layer but is vertically spread in the composited profile of Figure 4. As a result, the nocturnal vertical temperature gradients at the 10 m level are probably often seriously underestimated. A network of wind and temperature measurements indicates cold air drainage down the eastward descending slope, just west of the tower site. In the absence of cold air drainage, the subcanopy flow is generally from the south and the stratification above the understory is weaker.

The joint frequency distribution between the wind speed at 30 m and the temperature difference in canopy between 3m and 20m (Figure 6) indicates

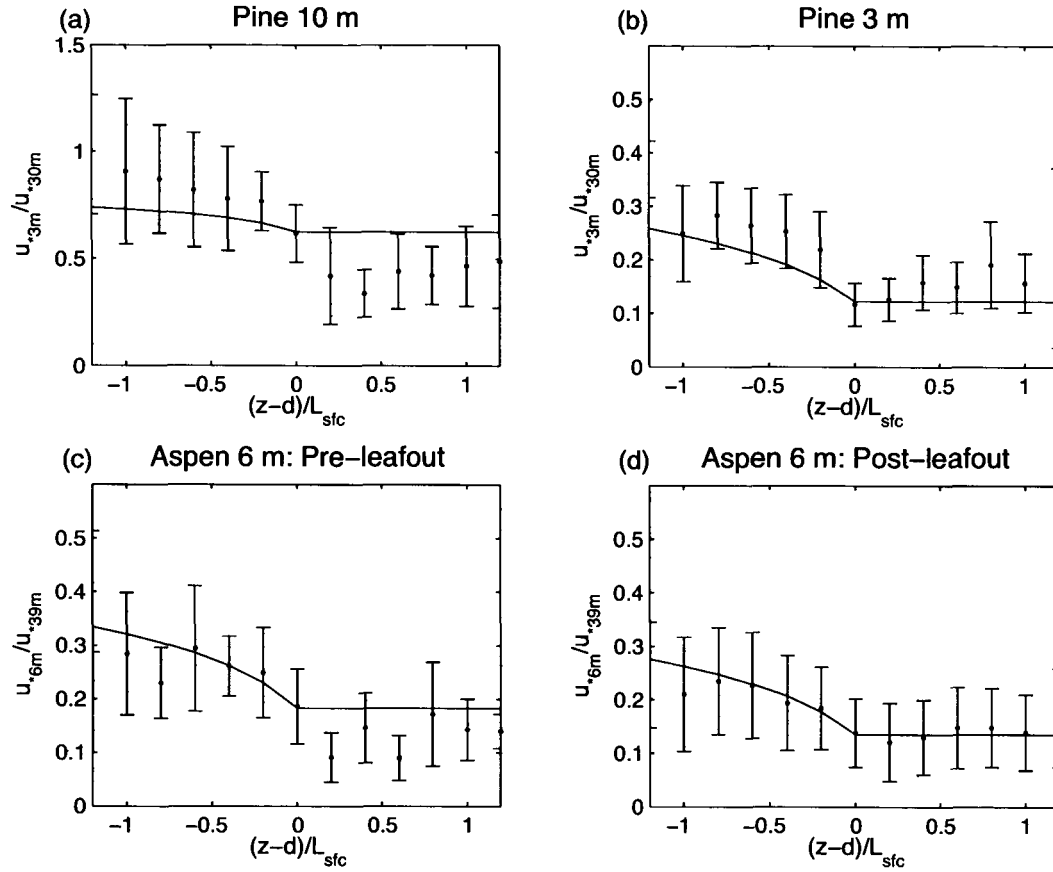


Figure 5: The ratio of friction velocities as a function of stability where  $L_{sfc}$  is the Obukhov length based on fluxes at the 39-m level, assumed to be in the surface layer. The solid line represents the prediction of the ratio based on the fit to Eq. 15 for unstable conditions and independent of the stability for stable conditions.

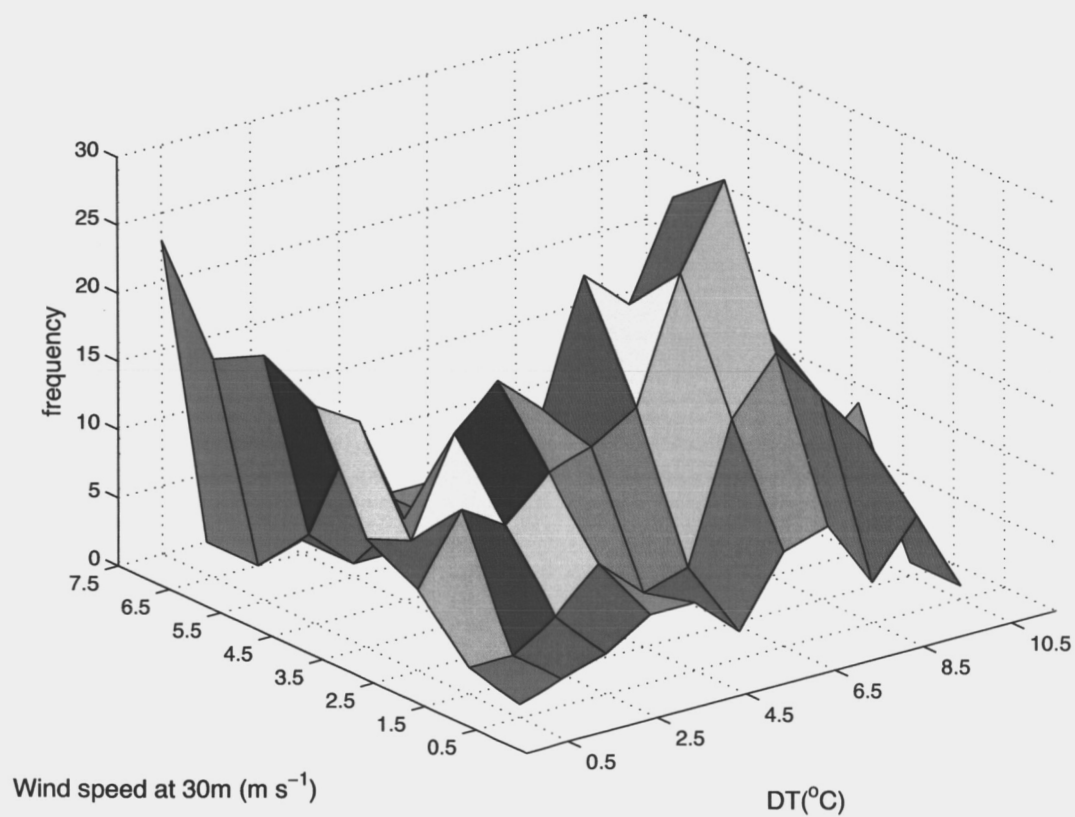


Figure 6: Joint frequency distribution of the 30 m wind speed and the canopy inversion strength between 3 and 20 m (DT) at the pine site. Color pattern is only for visualization.

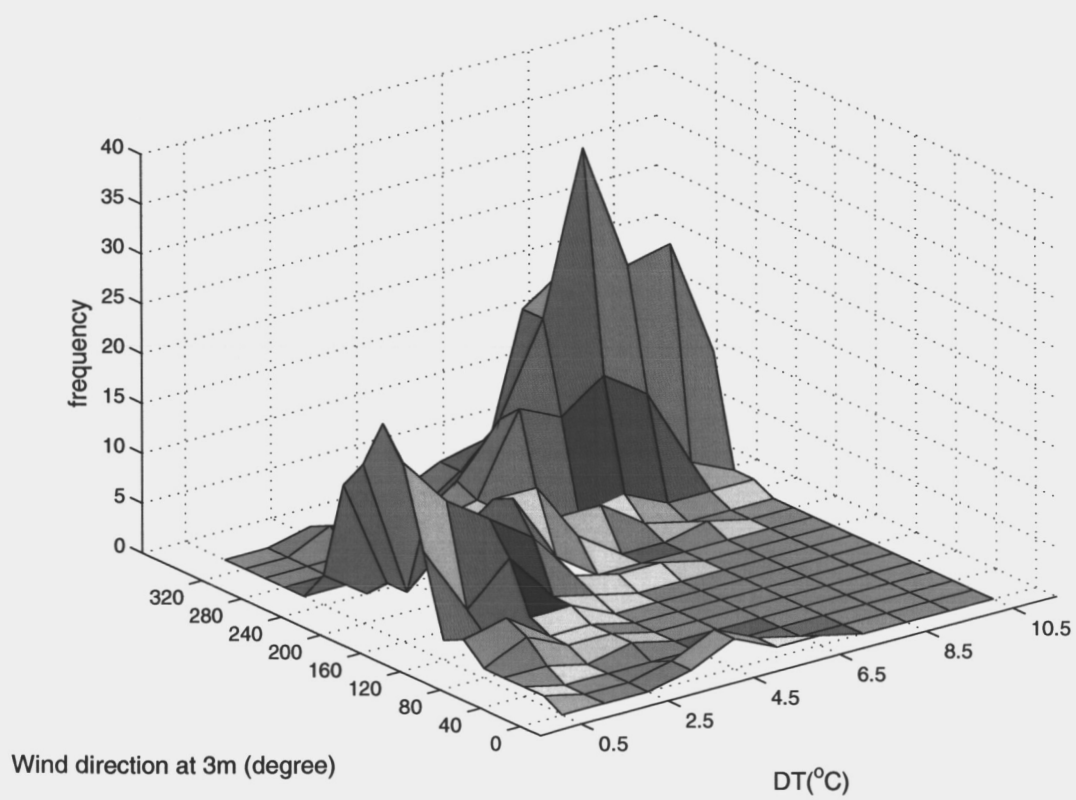


Figure 7: Joint frequency distribution of subcanopy 3-m wind direction and the canopy inversion strength between 3 and 20 m (DT) at the pine site.

that most of the nights with inversions greater than a few degrees occur with weak winds above the canopy and that strong winds generally correspond to weaker inversions of less than a few degrees. Almost all of the strong inversions occur with westerly subcanopy drainage flow. Weak canopy inversions correspond to southerly subcanopy flow more aligned with the flow above the canopy (Figure 7). The systematic development of subcanopy drainage flows and associated directional shear and strong inversions at the pine site probably account for much of the large scatter in the flux-gradient relationship. Inclusion of the directional shear associated with the drainage flow requires a separate momentum equation for the subcanopy.

## 6 Summary

The structure of turbulent transport within the canopy has been examined with eddy-correlation measurements from a relatively open ponderosa pine site and from an aspen site. The dependence of the nondimensional temperature gradient and mixing length for heat on stability approximately follow MO similarity theory even though the assumptions required for such similarity theory are not met. The nondimensional shear and mixing length for momentum deviate more from MO similarity. Deviations are most significant close to the top of the understory where the mixing coefficient depends much less on stability than would be estimated from the MO stability functions. Inclusion of the influence of subcanopy stability on subcanopy transfer is expected to improve formulation of transport of heat, momentum and presumably trace gases such as carbon dioxide.

Subcanopy drainage flows with strong capping inversions are common at the pine site and contribute to deviations from simple similarity theory. Accurate formulation of the within-canopy transport for these situations would



require a separate subcanopy momentum equation. We are collecting data with better vertical resolution to determine the influence of this inversion on decoupling between surface fluxes and fluxes above the canopy.

In spite of these difficulties and uncertainties with the above analyses, it is possible to improve upon existing simple formulations of within-canopy mixing, which completely neglect the dependence of within-canopy mixing on the stability. For example, an eddy diffusivity for heat has been constructed (Eq. 13) from the mixing length for neutral conditions (Eqs. 4, 5), the usual Monin-Obukhov stability functions and the formulation of the profile of the within-canopy friction velocity scale (Eqs. 14, 15), which depends on downward accumulated LAI and within-canopy stability.

More complete subcanopy flux profiles and their microscale variability are needed to provide more dependable profiles of the mixing length for heat and the dependence of the nondimensional shear on canopy architecture and within-canopy stability.

## ACKNOWLEDGMENTS

We gratefully thank Michael Unsworth, Reina Nakamura and Gaby Katul for their useful comments on the manuscript and Andy Black, Xuihui Lee and the rest of the BOREAS aspen team for the data from the aspen site. We also acknowledge Meredith Kurpius and John Wong for data collection at the pine site and Dean Vickers for data processing and flux calculations. This work was supported by Grant NAG5-11231 from the NASA Terrestrial Ecology Program, Grant FG0203ER63653 from the Department of Energy Terrestrial Carbon Program and Grant 0107617-ATM from the Physical Meteorology Program of the National Sciences Foundation

## References

- Albertson, J. D., Katul, G. G., Wiberg, P., 2001. Relative importance of local and regional controls on coupled water, carbon, and energy fluxes. *Adv. Water Res.*, 24, 1103-1118.
- Beljaars, A. C. M., and Holtslag, A. A. M., 1991. Flux parameterization over land surfaces for atmospheric models. *J. Appl. Meteorol.*, 30, 327-341.
- Blanken, P.D., Black, T. A., Yang, P. C., Neumann, H. H., Nesic, Z., Staebler, R., den Hartog, G., Novak, M. D., Lee X., 1997. Energy balance and canopy conductance of a boreal aspen forest: partitioning overstory and understory components. *J. Geophys. Res.* 102, 28915-28927.
- Blanken, P.D., Black, T. A., Neumann, H. H., den Hartog, G., Yang, P. C., Nesic, Z., Staebler, R., Chen, W. and Novak, M. D., 1998. Turbulent flux measurements above and below the overstory of a Boreal aspen forest. *Boundary-Layer Meteorol.* 89, 109-140.
- Bonan, G. B., 1996. A land surface model (LSM version 1.0) for ecological, hydrological and atmospheric studies: Technical description and user's guide. NCAR/TN-417+STR, NCAR Technical note.
- Brunet, Y. and Irvine, R., 2000. The control of coherent eddies in vegetation canopies: Streamwise structure spacing, canopy shear scale and atmospheric stability. *Boundary-Layer Meteorol.* 94, 139-163.
- Cheng, Y. and Brutsaert, W., 2005. Flux-profile relationships for wind speed and temperature in the stable atmospheric boundary layer. *Boundary-Layer Meteorol.*, 114, 519-538.
- Dyer, A.J., 1974. A review of flux-profile relationships, *Boundary-Layer Meteorol.*, 7, 363-372.
- Dwyer, M. J., Patton, E. G., Shaw, R. H., 1997. Turbulent kinetic energy budgets from a large eddy simulation of airflow above and within a forest canopy. *Boundary-Layer Meteorol.*, 84, 23-43.
- Finnigan, J., 2000. Turbulence in plant canopies. *Annu. Rev. Fluid. Mech.* 32, 519-571.

- Katul, G. G., Mahrt, L., Poggi, D. and Sanz, C., 2004. One- and two-equation models for canopy turbulence. *Boundary-Layer Meteorol.*, 113, 81-109.
- Lee, X., 1998. On micrometeorological observations of surface-air exchange over tall vegetation. *Agric. For. Meteorol.*, 91, 39-49.
- Mahrt, L., Lee, X., Black, A., Neumann, H. and Staebler, R. M., 2000. Vertical mixing in a partially open canopy. *Agric. For. Meteorol.*, 101, 67-78.
- Massman, W. J. and Weil, J. C., 1999. An analytical one-dimensional second-order closure model of turbulence statistics and the lagrangian time scale within and above plant canopies of arbitrary structure. *Boundary-Layer Meteorol.*, 91, 81-107.
- Nakamura, R. and Mahrt, L., 2001. Roughness lengths and similarity theory for local and spatially averaged fluxes. *Agric. For. Meteorol.*, 100, 47-61.
- Paw U, K. and Brunet, T., Y. Collinearu, Y. S., Shaw, R., Maitani, T., Qiu J. and Hipps, L., 1992. On coherent structure in turbulence above and within agricultural plant canopies. *Agric. For. Meteorol.*, 61, 55-68.
- Poggi, D., Katul, G. G. and Albertson, J. D., 2004. Momentum transfer and turbulent kinetic energy budgets within a dense model canopy. *Boundary-Layer Meteorol.* 111, 589-614.
- Raupach, M. R., 1994. Simplified expressions for vegetation roughness length and zero-plane displacement as function of canopy height and area index. *Boundary-Layer Meteorol.*, 71, 211-216
- Raupach, M. R., Finnigan, J. J., Brunet, Y., 1996,. Coherent eddies and turbulence in vegetation canopies: Mixing-layer analogy. *Boundary-Layer Meteorol.*, 78, 351-382.
- Shaw, R. H. and Schumann, U., 1992. Large-eddy simulation of turbulent flow above and within a forest. *Boundary-Layer Meteorol.* 61, 47-64.
- Schwarz, P., Law, B., Williams, M., Irvine, J., Kurpius, M., and Moore, D., 2004. Climatic versus biotic constraints on carbon and water fluxes in seasonally drought-affected ponderosa pine ecosystems. *Global Biochem. Cycles* 18, GB4007, doi:10.1029/2004GB002234.
- Sellers, P., Hall, F., Margolis, H., Kelly, B., Baldocchi, D., den Hartog, G., Cihlar, F., Ryan, M. G., Goodison, B., Crill, P., Ranson, K. J., Lettenmaier, D.,

- and Wickland, D. E., 1995. The Boreal Ecosystem - Atmosphere study (BOREAS): An overview and early results from the 1994 field Year. *Bull. Amer. Meteorol. Soc.*, 76, 1549-1577.
- Shuttleworth, W. J., and Wallace, J. S., 1985. Evaporation from sparse crops - An energy combination theory. *Quart. J. Roy. Meteorol. Soc.*, 111, 839-855.
- Wilson, J. D., Finnigan, J. J., and Raupach, M. R., 1998. First-order closure for plant canopy flows. *Quart. J. Roy. Meteorol. Soc.*, 124, 705-732